

A MODELING STUDY OF LOW-FREQUENCY CSEM IN SHALLOW WATER

Michael A. Frenkel and Sofia Davydycheva
EMGS ASA

ABSTRACT

The applicability and resolution power of low-frequency Controlled-Source Electromagnetic (CSEM) data in shallow and deep water environments are studied on typical CSEM benchmark models. We apply the fast and accurate 3D finite-difference (FD) modeling code. The FD scheme is solved iteratively using the multi-frequency Spectral Lanczos Decomposition Method. We showed that use of low-frequency ($f < 0.05$ Hz) electromagnetic measurements can overcome the airwave effect, allowing CSEM technology to be effectively used in shallow water to resolve deep 3D resistive targets.

Introduction

The offshore frequency-domain CSEM method can be effectively used to find, test and evaluate hydrocarbon reservoirs (Eidesmo et al., 2002; Srnka et al., 2006; Dell'Aversana et al., 2007). It has been shown that the method works well when applied in waters in excess of a few hundred meters at frequencies ranging from 0.1 to 10 Hz. In water depths less than 300 m, air wave effects can become significant (Mittet et al, 2004; Dell'Aversana, 2007; Weiss, 2007; Mittet, 2008). In many cases, particularly where the seabed is relatively flat, traditional techniques such as up-down separation (Amundsen et al., 2006) or modeling-based data correction (Lu et al., 2007) can effectively eliminate the air wave. However, as CSEM expands the application window into even shallower water (30-100 m), the airwave effect can still prevent reliable detection of small buried resistors. In this paper, we perform a modeling study of low-frequency CSEM responses. This analysis suggests that low-frequency domain CSEM technology can be used in very shallow water to overcome the air wave effect and resolve 3D resistive targets.

Modeling Methodology and Benchmarking

The motivation for this study is to evaluate the CSEM responses generated by a relatively small reservoir in shallow and deep water settings. Fig. 1 illustrates the XZ cross-sections of the models used in this study. The 1D model (a) presents an infinite reservoir propagated in the X and Y-directions in the presence of shallow water (depth 200 m), whereas in the 3D model cases (b), the reservoir width in the X and Y-directions is 2 km. In the 2.5D case, the reservoir length along Y-direction is set to a large number (50 km). In all model cases, water, background, and target resistivities are 0.3, 1.0, and 50 $\Omega\cdot\text{m}$, respectively. In the 1D tests, the target depth (TD) is 1 km; in the 2.5D and 3D models, TD is 600 m or 1 km or 2 km.

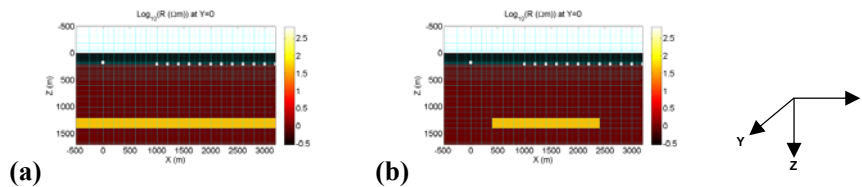


Figure 1: XZ cross-sections of 1D (a) and 2.5D/3D (b) formation models at $Y=0$. The color bar represents resistivity range on \log_{10} scale, and the model accordingly consists of air (white), sea water (black), earth below the seafloor (brown), target reservoir (yellow). The white dots are the X-directed Horizontal Electric Dipole (HED) source (leftmost white dot) and a group of equally-spaced receivers. The blue lines are the finite-difference (FD) grid.

In this paper, we apply the 3D finite-difference (FD) modeling code developed by Davydycheva and Druskin (1995). This approach entails solving Maxwell's equations discretized on a FD grid. The FD scheme is solved iteratively using the multi-frequency Spectral Lanczos Decomposition Method (SLDM). The code was validated against 1D quasi-analytical solutions. In Fig. 2, magenta curves present the dipole-dipole response at $f=0.05$ Hz to the model of an infinite reservoir depicted in Fig. 1a.

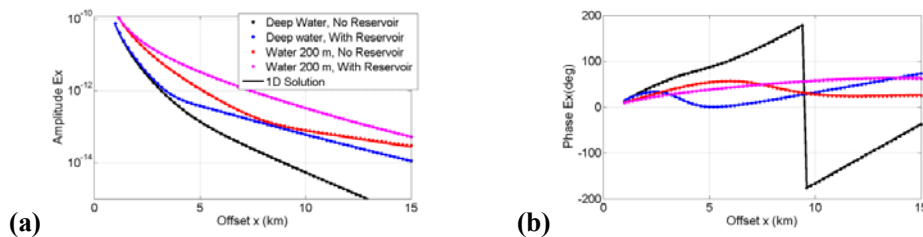


Figure 2: Comparison of 3D modeling results against 1D solutions for the model of a 600 m deep reservoir in deep and shallow (200 m) water: (a) E_x magnitude, (b) E_x phase difference.

One can see a good agreement between the FD (dots) and 1D (lines) solutions for all offsets and for both the amplitude (Fig. 2a) and phase difference (Fig. 2b). Red curves correspond to the case without the reservoir. Blue/black curves present the deep-water solution with/without the reservoir, respectively.

Synthetic Examples

Wavelength. Spatial resolution of CSEM measurements at very low frequencies (near-DC case) is primarily determined by offsets and at high frequencies by the EM field wavelength (λ). At the CSEM - low frequency range, λ is related to the plane-wave skin-depth, δ : $\lambda = 2\pi\delta$, $\delta = (\rho/(\mu_0\pi f))^{1/2}$, where ρ , f , and μ_0 are resistivity, frequency, magnetic permeability of free space, respectively. The table below shows δ and λ for three frequencies and $\rho = 1 \Omega\cdot\text{m}$:

f (Hz)	δ (m)	λ (m)
0.05	2251	14143
0.25	1007	6327
1.00	503	3160

1D Case. In shallow water (Fig. 3a), the anomalous reservoir response is weak at high frequencies, but it is stronger at near-DC frequencies (e.g., <0.05 Hz), at which the airwave effect is weak. In deep water (Fig. 3b), the anomalous response is stronger at higher frequencies. However, the signal attenuates at higher frequencies, and its level at longer offsets becomes closer to the noise floor, which makes these data difficult to interpret/invert.

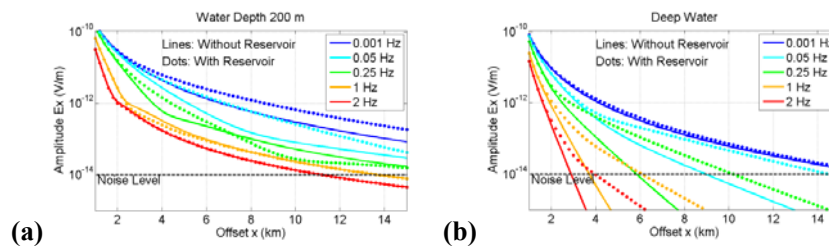


Figure 3: Comparison of E_x magnitude for 1D model with (dotted lines) and without (solid lines) the target reservoir for a wide range of frequencies ranging from 0.001 to 2.0 Hz. The anomalous reservoir response can be estimated as the difference between the dotted and solid curves of the same color. Left (a) and right (b) are the shallow (200 m) and the deep water cases, respectively.

2.5D Case. To illustrate the resolution of CSEM in shallow and deep water at low frequencies, we chose two positions of the reservoir at 1 km (Fig. 4) and 2 km (Fig. 5) below the seafloor. Figs. 4-5 show the E_x component normalized to a reference measurement located far from the reservoir and its absolute amplitude. The results presented in Fig. 4 illustrate that in deep water, the normalized response is stronger at higher frequency, whereas in shallow water, it is stronger at lower frequency. These effects are more apparent at offsets longer than 2 km. However, due to signal attenuation at higher frequencies and longer offsets, it is impractical to use these data in deep water.

Note that in the model cases with the target at 1 km depth (Fig. 4), the “width” of the reservoir response (estimated by the distance between the inflection points on the normalized E_x curve flanks) is roughly the same for all the frequencies and is determined primarily by the offset. The reason is that the signal wavelength λ below the seafloor is equal or greater than the offset at the considered range of frequencies.

The results presented in Fig. 5 display ~20% anomalous effect from the 2 km deep target at 50 m water depth and $f \leq 0.05$ Hz. The feasibility of resolving deep targets using low-frequency CSEM data should be further investigated using inversion-based methods (e.g., Zach et al., 2008).

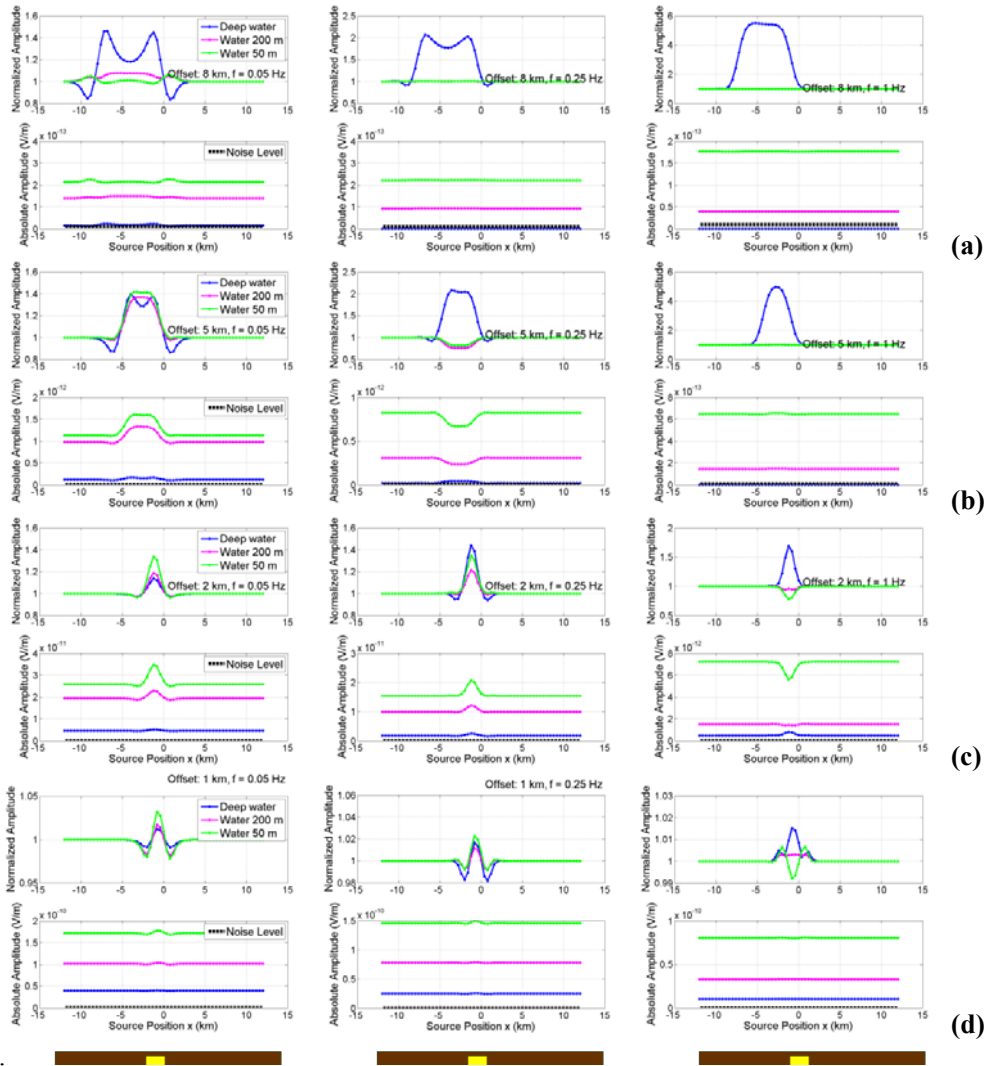


Figure 4: E_x data at 0.05, 0.25 and 1 Hz at 8 km (a), 5 km (b), 2 km (c) and 1 km (d) offsets. The normalized and absolute amplitudes for each offset are in the top and bottom row of figs. a-d. The yellow box indicates the lateral position and size of the reservoir located 1 km below the seafloor.

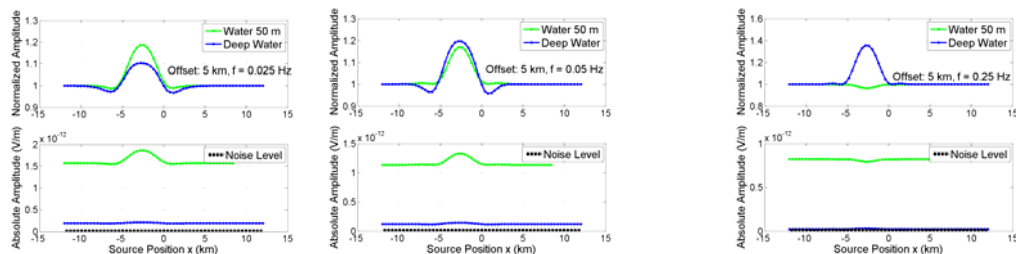


Figure 5: E_x data for the model of 2 km deep reservoir at $f = 0.025, 0.05,$ and 0.25 Hz at 5 km offset.

Comparison of 2.5D and 3D Cases. Here we present the modeling results comparison for 2.5D and 3D models. The 3D model contains a 50 Ω -m reservoir located at 600 m below the seafloor. The 3D reservoir has dimensions $(X \times Y \times Z) = (2000 \times 2000 \times 200)$ m, whereas in the 2D model, model properties are Y-invariant. The results are shown in Fig. 6. At 2 km offset, there is no significant difference between the two responses, and the resolution power of the

CSEM does not depend much on frequency. It should be noted that at 5 km offset, the 3D response is approximately two times lower than the 2.5D response. These observations suggest that fast 2.5D modeling can be used for a qualitative 3D data analysis.

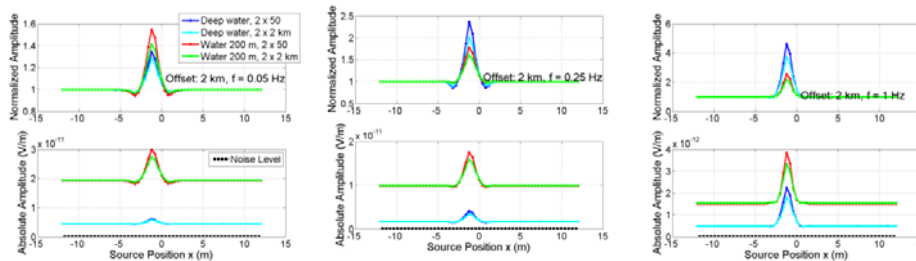


Figure 6: Comparison of modeling results using 2.5D and 3D models. E_x data shown for shallow and deep water cases at 0.05, 0.25 and 1 Hz for 2 km offset. Reservoir depth is 600 m below the seafloor.

Conclusions and Recommendations

Using an efficient 3D forward modeling method applied to a CSEM benchmark model, we found that use of low-frequency ($f < 0.05$ Hz) electromagnetic measurements can overcome the airwave effect, allowing CSEM technology to be used in water as little as 50 m deep. The selection of optimal excitation frequency should be based on the target and background formation parameters and also on the water depth. Additional modeling studies and field tests in a variety of shallow water environments are recommended.

Acknowledgements

The authors are indebted to EMGS for granting permission to publish this work. We would like to express our special thanks to Bjarte Bruheim and Dave Ridyard for support throughout this study; Frank Maaø, Friedrich Roth and Juergen Zach for valuable suggestions.

References

- Amundsen, L., Løseth, L., Mittet, R., Ellingsrud, S., and Ursin, B. [2006] Decomposition of electromagnetic fields into upgoing and downgoing components, *Geophysics*, 71, G211-223.
- Davydycheva, S. and Druskin, V. [1995] Staggered grid for Maxwell's equations in arbitrary 3-D inhomogeneous anisotropic media. *Proc. Int. Symp. on Three-Dimensional Electromagnetics, Schlumberger-Doll Research, Ridgefield, CT*, 181–187.
- Dell'Aversana, P. [2007] Improving interpretation of CSEM in shallow water, *TLE*, 332-335.
- Dell'Aversana, P., Vivier, M., and Tansini, A. [2007] Expanding the frequency spectrum in marine CSEM applications. *EGM Workshop, Capri, Italy*.
- Eidesmo, T., Ellingsrud, S., MacGregor, L.M., Constable, S., Sinha, M.C., Johansen, S., Kong, F.N. and Westerdahl, H. [2002] Sea Bed Logging (SBL), a new method for remote and direct identification of hydrocarbon filled layers in deepwater areas, *First Break*, 20(3), 144-152.
- Lu, X., Srnka, L., and Carazzone, J. [2007] Method for removing air wave effect from offshore frequency domain controlled-source electromagnetic data, US patent 7,277,806 B2.
- Mittet, R., Løseth, L., and Ellingsrud, S. [2004] Inversion of SBL data acquired in shallow water. *66th EAGE Conference and Exhibition*, Extended abstracts, E020.
- Mittet, R. [2008] Normalized amplitude ratios for frequency-domain CSEM in very shallow water. *First Break*, 26(11), 47-54.
- Srnka, L.J., Carazzone, J.J., Ephron, M.S. and Eriksen, E.A. [2006] Remote reservoir resistivity mapping. *TLE*, 25, 972–975.
- Weiss J., [2007] The fallacy of the “shallow-water problem” in marine CSEM exploration, *Geophysics*, 72, A93-97.
- Zach, J.J., Bjørke, A.K., Støren, T., and Maaø, F. [2008] 3D inversion of marine CSEM data using a fast finite-difference time-domain forward code and approximate Hessian-based optimization. *SEG 2008 Expanded Abstracts*, Las Vegas, NV, USA.